



Effects of high-field electrical stress on the conduction properties of ultrathin La₂O₃ films

E. Miranda, J. Molina, Y. Kim, and H. Iwai

Citation: [Applied Physics Letters](#) **86**, 232104 (2005); doi: 10.1063/1.1944890

View online: <http://dx.doi.org/10.1063/1.1944890>

View Table of Contents: <http://scitation.aip.org/content/aip/journal/apl/86/23?ver=pdfcov>

Published by the [AIP Publishing](#)



Re-register for Table of Content Alerts

Create a profile.



Sign up today!



Effects of high-field electrical stress on the conduction properties of ultrathin La_2O_3 films

E. Miranda^{a)}

Departament d'Enginyeria Electrònica, Universitat Autònoma de Barcelona, Edifici Q,
08193 Bellaterra, Spain

J. Molina, Y. Kim, and H. Iwai

Frontier Collaborative Research Center, Tokyo Institute of Technology, 4259, Nagatsuta, Midori-ku,
Yokohama 226-8502, Japan

(Received 16 November 2004; accepted 27 April 2005; published online 3 June 2005)

Electron transport in high-field stressed metal-insulator-silicon devices with ultrathin (<5 nm) lanthanum oxide layers is investigated. We show that the leakage current flowing through the structure prior to degradation is direct and Fowler-Nordheim tunneling conduction, while that after stress exhibits diode-like behavior with series and parallel resistances. In this latter case, a closed-form expression for the current-voltage characteristic, based on the Lambert W function, is presented. Current evolution from one regime to the other during constant voltage stress takes place by means of discrete current steps of nearly identical magnitude, which would be indicative of the occurrence of multiple dielectric breakdowns across the insulating layer. © 2005 American Institute of Physics. [DOI: 10.1063/1.1944890]

High-dielectric constant (high- K) materials are currently being extensively investigated because of their potential capabilities to replace silicon dioxide (SiO_2) as the gate insulator in complementary metal-oxide-semiconductor (CMOS) technologies.¹ The main point in using high- K dielectrics resides in the fact that these materials allow reducing the gate tunneling current, and therefore standby power consumption, while keeping the equivalent oxide thickness as required for device scaling. Among the large list of possible high- K s, lanthanum oxide (La_2O_3) seems to be a promising candidate that has attracted the attention of many research groups worldwide.^{2–10} It is worth pointing out that La_2O_3 films are considered not only for its high dielectric constant ($K \approx 27^{8–10}–30^1$), but also because the large band gap ($E_G \approx 4.3^1–5.5^6$ eV), the good thermodynamic stability (lattice energy of 12 687 kJ/mol) in contact with silicon substrates,^{2,6} and the compatibility with standard microelectronic fabrication processes.⁵ Even though the electron transport in La_2O_3 has been the subject of previous reports,^{5,8–10} no consensus has been reached about the physical mechanisms involved likely due to the variability of the material properties with deposition techniques and growth conditions. In this work, we show that, in a first stage, our samples exhibit a current dependence compatible with the tunneling mechanism. According to our analysis, for low applied voltages (<1 V) the current is due to direct tunneling (DT), in agreement with the experimental and simulation results of Yeo *et al.*,⁹ whereas for higher biases the current is due to Fowler-Nordheim (FN) injection corrected for a series resistance effect. Next, this latter regime is used to stress the sample until breakdown and the resulting current-voltage (I - V) characteristic analyzed within the framework of a diode-like conduction model. If the sample is stressed even further, a new leakage mechanism in parallel with the previous one comes into play. We present a compact model able to reproduce with a high degree of accuracy the essential fea-

tures exhibited by the conduction characteristics of La_2O_3 under such circumstances. Additionally, we show that during a constant voltage stress the current evolves in a stepwise manner, revealing the presence of weak spots in the dielectric layer.

For the experiments we used capacitors with oxide thicknesses of 3.3 nm. La_2O_3 films were deposited on chemically cleaned n -type Si (100) substrates ($0.02–0.8 \Omega \text{ cm}$) by electron beam evaporation at 250°C . The pressure in the chamber during the deposition was 10^{-9} Torr. The films were annealed in dry- N_2 for 5 min at 400°C . The physical thicknesses were determined by an ellipsometer Otsuka FE-5000. Finally, electrodes with area $7.85 \times 10^{-5} \text{ cm}^2$ were deposited by Al evaporation through a shadow mask. Electrical measurements were performed at dark conditions and room temperature using a semiconductor parameter analyzer HP4156B. The voltage ramp rate was about 1 V/s with a voltage stepsize of 5 mV. The sampling rate for the current-time measurements was 50 ms. Figure 1 shows typical I - V characteristics measured before and after degradation. In this particular case, the lower characteristic, i.e., that ascribed to tunneling conduction, has been used to stress the sample. Notice that, even though the whole characteristic is shown for comparison purposes, only that part of the curve corresponding to the highest fields causes the major damage to the sample. In order to confirm that this is indeed tunneling conduction, Fig. 2 shows the so-called FN plot corrected for a series resistance effect. As it is well known, FN conduction corresponds to a straight line in this plot. As proposed in Ref. 11, we consider that the effective potential drop over the insulating layer is $V - IR_{\text{FN}}$, where V is the applied voltage, I the current and R_{FN} a series resistance. The procedure to obtain R_{FN} consists of minimizing the linear correlation coefficient associated with the transformed data in the range from 1.1 to 2.5 V. R_{FN} plays no role in the DT region. The solid line in Fig. 2 corresponds to Schuegraf's tunneling model.¹² For this measurement we have found $R_{\text{FN}} = 45.8 \Omega$, and the tunneling parameters $m^* = 0.15m$, $\Phi = 2.2$ eV, where

^{a)}Electronic mail: enrique.miranda@uab.es

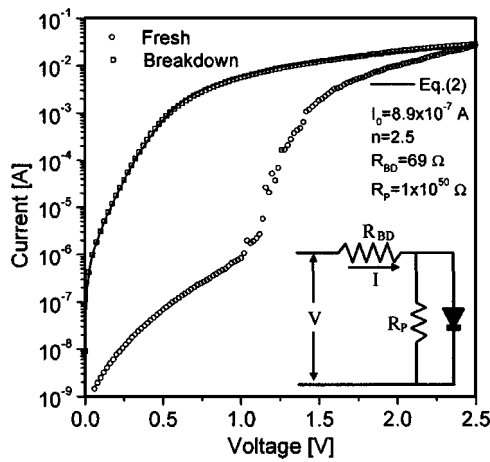


FIG. 1. Current–voltage characteristics before and after electrical stress. Symbols correspond to experimental data and the solid line to fitting results using Eq. (2). The inset shows the equivalent electrical circuit proposed to deal with the post-breakdown current.

m^* , m , and Φ are the electron effective mass in the insulator, the free electron mass and the cathode barrier height, respectively. Although the barrier height is in close agreement with a previously reported value ($\Phi=2.3$ eV), the effective mass is somewhat smaller ($m^*=0.26m$).⁹ Our effective mass is closer to the values found for other high- K dielectrics, such as Al_2O_3 ($m^*=0.11m$) and HfO_2 ($m^*=0.18m$).^{13,14} However, after the high-field voltage sweep, a completely different characteristic is observed (see Fig. 1). The large leakage current is now attributed to the local loss of the insulating property of the La_2O_3 film. It does not scale with the device area neither with the oxide thickness, which is consistent with the random and local nature of electron transport. From 0 to 0.7 V, the current depends exponentially on the applied voltage, whereas for higher voltages it behaves linearly. Based on this observation, in order to simulate such I – V characteristics, we propose an equivalent electrical circuit formed by a diode with series and parallel resistances. The introduction of a parallel resistance will be explained later. According to the configuration shown in the inset of Fig. 1, the current is expressed as:

$$I = I_0 \left[\exp\left(\frac{V - IR_{BD}}{nV_T}\right) - 1 \right] + \frac{V - IR_{BD}}{R_P}, \quad (1)$$

where I_0 is a constant often referred to as the reverse saturation current, n is called the ideality factor, $V_T \approx 0.026$ mV is the thermal voltage at room temperature and R_{BD} and R_P are the postbreakdown series and parallel resistances, respectively. Equation (1) is an implicit equation for the current that can be solved in terms of the Lambert W function, i.e., the solution of the equation $W \exp(W) = x$. The final expression for the current as a function of the applied voltage reads:¹⁵

$$I = \frac{nV_T}{R_{BD}} W \left\{ \frac{I_0 R_{BD} R_P}{nV_T (R_{BD} + R_P)} \exp\left[\frac{R_P (V + I_0 R_{BD})}{nV_T (R_{BD} + R_P)}\right] \right\} + \frac{V - I_0 R_P}{R_{BD} + R_P}. \quad (2)$$

In Fig. 1, we show a fitting (solid line) to a typical I – V characteristic obtained after a single voltage-ramp test (from 0 to 2.5 V). The parameters used in Eq. (2) are $I_0 = 8.9 \times 10^{-7}$ A, $n = 2.5$, and $R_{BD} = 69 \Omega$. At this stage, the parallel resistance plays no role and, for practical purposes, the corresponding circuit branch can be regarded as an open circuit. Notice that the ideality factor $n = 2.5$ is somewhat higher than those found in “macroscopic” diodes, which are commonly in the range $1 < n < 2$. In this regard, one should be aware that we are not dealing with a well-defined junction but with a sort of constriction connecting both electrodes, be it in the form of a percolation path or simply a trap strategically located within the insulator, as suggested for other high- K dielectrics.¹⁶ Among the many factors that yield ideality factors greater than unity we can mention the presence of an interfacial layer,¹⁷ the recombination of electrons and holes,¹⁸ and size effects of quantum nature.¹⁹

Now, if the sample is further stressed, for instance using successive voltage ramps or by the application of a constant voltage to the gate, a new current component becomes visible. This leakage current flows in parallel with the diode-like mechanism discussed above and is only detectable for very low biases (< 0.3 V). To model this component, we have assumed an ohmic path between the electrodes represented by the parallel resistance R_P , as shown in the inset of Fig. 1. We have found that R_P is in general in the order of several k Ω s and the effect of neglecting this resistance is clearly illustrated in Fig. 3, where log-log axes were used in order to magnify the voltage region of interest. For this particular measurement we have found $R_P = 3.3$ k Ω and $R_{BD} = 26 \Omega$. In junction diodes, the excess current at low bias is commonly ascribed to a generation-recombination mechanism in the depletion region.²⁰ Although it is somewhat speculative at this stage to connect that problem with ours, recombination-assisted electron transport²¹ and interface charge trapping²² have been proposed to explain the stress-induced leakage current increase at low fields in SiO_2 . As it is expected for a more degraded structure, the breakdown resistance is lower than that obtained after the first voltage-ramp (see Fig. 1). This is in agreement with the fact that the constriction resistance depends, roughly speaking, on the inverse of the damaged area.²³

Particularly noteworthy is the manner in which the current evolves from the FN to the postbreakdown regime during a constant voltage stress. As shown in Fig. 4, the transi-

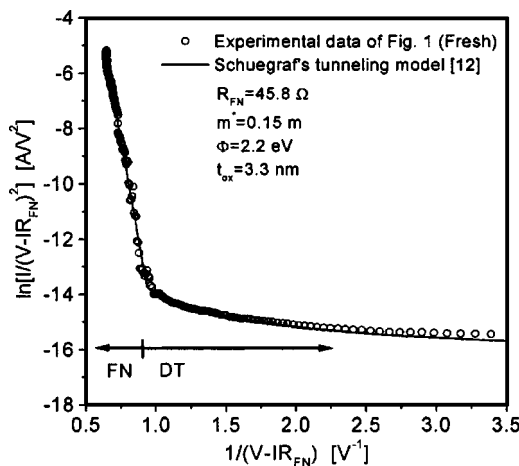


FIG. 2. Fowler-Nordheim plot associated with the experimental data (symbols) shown in the lower curve of Fig. 1. The solid line corresponds to Schuegraf's tunneling model (Ref. 12). FN and DT refer to the Fowler-Nordheim and direct tunneling regimes, respectively.

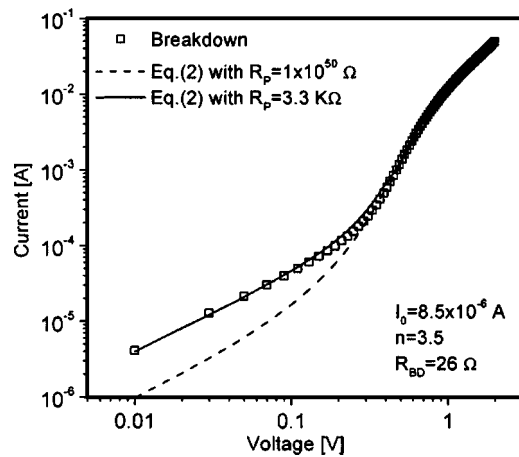


FIG. 3. Log-log plot of a current–voltage characteristic after a prolonged high-field electrical stress. Symbols are experimental data and the lines are obtained using Eq. (2). Notice the effect of taking into account the parallel resistance R_p .

tion is not gradual but in the form of discrete steps (≈ 0.4 mA at 2 V), indicating that the final current is the result of many leakage sites each one contributing approximately with the same amount of current. This behavior closely resembles the phenomenon of successive dielectric breakdowns in SiO_2 ²⁴ and a similar stepwise current increase has been observed in HfSiON .¹⁶ In order to show that the damage caused to the structure is permanent, the same sample was stressed twice, first for about 8 s and second for 15 s. As can be seen in Fig. 4, when the test is resumed, the

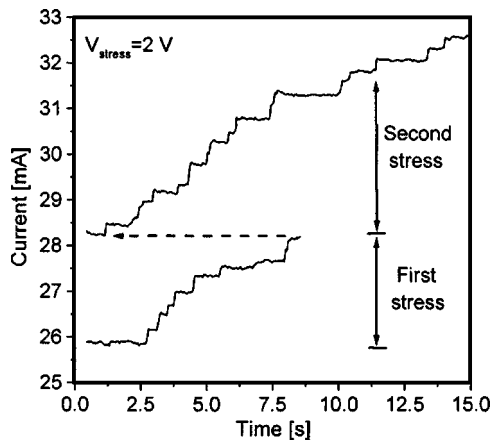


FIG. 4. Time-dependent breakdown characteristics during a constant voltage stress at 2 V. The lower curve corresponds to a first stage of degradation. Then, a second stress is applied to the same sample. The arrow indicates the connection between both runs.

current starts at the same final level reached after the first degradation stage.

In summary, we have found that after a high-field Fowler-Nordheim stress, the leakage characteristics of capacitors with ultrathin La_2O_3 films can be simulated using a diode-like model with series and parallel resistances. A prolonged stress leads to the appearance of multiple leakage sites of nearly identical characteristics, which may be indicative of the existence of a large number of weak spots in the oxide layer.

This work was supported by the Semiconductor Technology Academic Research Center (STARC), MEXT-Special Coordination Funds for Promoting Science and Technology, Matsumae International Foundation (Japan), and Ministerio de Ciencia y Tecnología (Spain) under Project No. TIC2003-08213-C02.

- ¹G. Wilk, R. Wallace, and J. Anthony, *J. Appl. Phys.* **89**, 5243 (2001).
- ²K. Hubbard and D. Schlom, *J. Mater. Res.* **11**, 2757 (1996).
- ³A. Chin, Y. Wu, S. Chen, C. Liao, and W. Chen, *Symposium-on VLSI Technology 2000*, p. 16.
- ⁴S. Guha, E. Cartier, M. Gribelyuk, N. Bojarczuk, and M. Copel, *Appl. Phys. Lett.* **77**, 2710 (2000).
- ⁵J. Jun, D. Choi, K. Kim, K. Oh, and C. Hwang, *Jpn. J. Appl. Phys., Part 1* **42**, 3519 (2003).
- ⁶S. Ohmi, C. Kobayashi, I. Kashiwagi, C. Ohshima, H. Ishiwara, and H. Iwai, *J. Electrochem. Soc.* **150**, F134 (2003).
- ⁷S. Stemmer, J. Maria, and I. Kingon, *Appl. Phys. Lett.* **79**, 102 (2001).
- ⁸Y. Wu, M. Yang, A. Chin, W. Chen, and C. Kwei, *IEEE Electron Device Lett.* **21**, 341 (2000).
- ⁹Y. Yeo, T. King, and C. Hu, *Appl. Phys. Lett.* **81**, 2091 (2002).
- ¹⁰Y. Kim, S. Ohmi, K. Tsutsui, and H. Iwai, *Proceedings of European Solid-State Device Research Conference 2004*, p. 81.
- ¹¹E. Miranda, *Electron. Lett.* **40**, 1153 (2004).
- ¹²K. Schuegraf and C. Hu, *IEEE Trans. Electron Devices* **41**, 761 (1994).
- ¹³S. Huang and J. Hwu, *IEEE Trans. Electron Devices* **50**, 1658 (2003).
- ¹⁴Y. Hou, M. Li, H. Yu, and D. Kwong, *IEEE Electron Device Lett.* **24**, 96 (2003).
- ¹⁵A. Ortiz-Conde, F. García Sanchez, and J. Muci, *Solid-State Electron.* **44**, 1861 (2000).
- ¹⁶M. Koyama, H. Satake, M. Koike, T. Ino, M. Suzuki, R. Iijima, Y. Kamimuta, A. Takashima, C. Hongo, and A. Nishiyama, *IEEE Proc. Int. Electron Device Meeting (2003)*, p. 931.
- ¹⁷H. Card and E. Rhoderick, *J. Phys. D* **4**, 1602 (1971).
- ¹⁸H. Henish, *Semiconductor Contacts* (Clarendon, Oxford, 1984).
- ¹⁹G. Smit, S. Rogge, and T. Klapwijk, *Appl. Phys. Lett.* **81**, 3852 (2002).
- ²⁰G. Neudeck, *The PN Junction Diode, Modular Series on Solid Devices* (Addison-Wesley, Reading, MA, 1989), Vol. 2.
- ²¹D. Ielmini, A. Spinelli, and A. Lacaita, *Appl. Phys. Lett.* **76**, 1719 (2000).
- ²²C. Huang and J. Hwu, *J. Appl. Phys.* **89**, 5497 (2001).
- ²³T. Bearda, P. Woerlee, H. Wallinga, and M. Heyns, *Jpn. J. Appl. Phys., Part 1* **41**, 2431 (2002).
- ²⁴J. Suñé, E. Wu, and W. Lai, *IEEE Trans. Electron Devices* **51**, 1584 (2004).